



HAL
open science

Measurements and calculations of collisional line broadening and mixing in the Raman spectrum of N₂ perturbed by CO

Denis Paredes-Roibas, Raul Z. Martinez, Franck Thibault

► **To cite this version:**

Denis Paredes-Roibas, Raul Z. Martinez, Franck Thibault. Measurements and calculations of collisional line broadening and mixing in the Raman spectrum of N₂ perturbed by CO. *Journal of Quantitative Spectroscopy and Radiative Transfer*, 2023, 302, pp.108560. 10.1016/j.jqsrt.2023.108560 . hal-04057328

HAL Id: hal-04057328

<https://hal.science/hal-04057328>

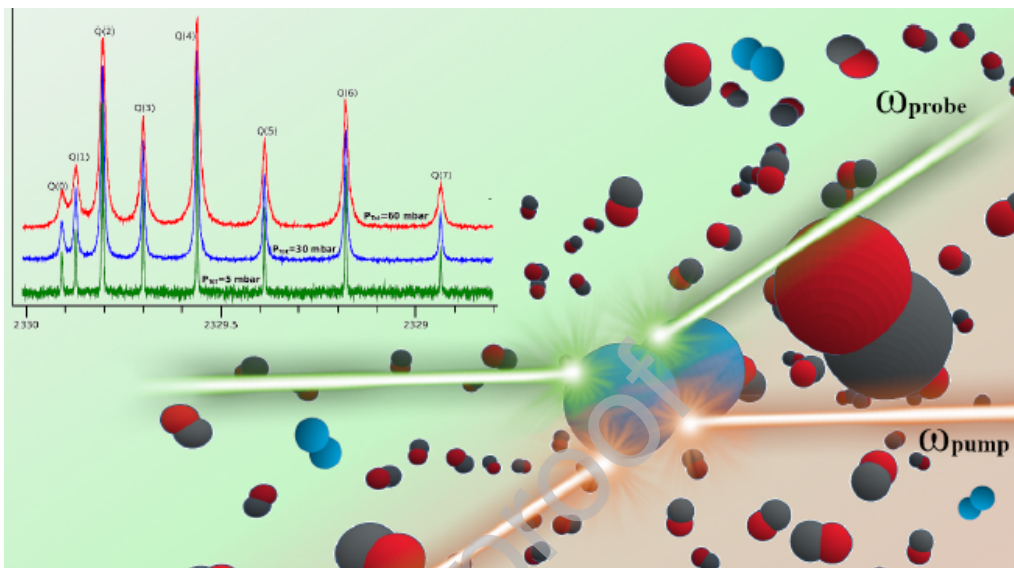
Submitted on 15 May 2023

HAL is a multi-disciplinary open access archive for the deposit and dissemination of scientific research documents, whether they are published or not. The documents may come from teaching and research institutions in France or abroad, or from public or private research centers.

L'archive ouverte pluridisciplinaire **HAL**, est destinée au dépôt et à la diffusion de documents scientifiques de niveau recherche, publiés ou non, émanant des établissements d'enseignement et de recherche français ou étrangers, des laboratoires publics ou privés.



Distributed under a Creative Commons Attribution - NonCommercial 4.0 International License






Highlights:

- Joint theoretical and experimental lineshape study in the rovibrational isotropic Raman spectrum of N₂ in a bath of CO between 77 and 298 K.
- Determination of collisional broadening coefficients and line mixing coefficients
- Two different theoretical approaches have been explored: a quantum dynamical calculation and a parametric one utilizing the energy-corrected sudden (ECS) approximation.
- Comparison of experimental vs.theoretical results and evaluation of the effect of the different approximations used in the calculations.

Journal Pre-proof

Measurements and calculations of collisional line broadening and mixing in the Raman spectrum of N₂ perturbed by CO.

Denís Paredes-Roibás ^{a,b}, Raúl Z. Martínez ^a, Franck Thibault ^c


^a*Instituto de Estructura de la Materia, IEM-CSIC. Serrano 123, 28006 Madrid, Spain*

^b*Departamento de Ciencias y Técnicas Fisicoquímicas, Facultad de Ciencias, Universidad Nacional de Educación a Distancia (UNED), Campus de Las Rozas. Avenida de Esparta, 9. Ctra. de las Rozas al Escorial Km. 5 (Urb. Monterozas) 28232 Las Rozas, Madrid, Spain*

^c*Univ Rennes, CNRS, IPR (Institut de Physique de Rennes)-UMR 6251,F-35000 Rennes, France*

Abstract

Measurements in the rotationally-resolved Q branch of the Raman spectrum of the fundamental vibration ($v = 0 \rightarrow v = 1$) of N₂ perturbed by CO have been conducted at three temperatures, 77, 195 and 298 K, in order to obtain broadening and mixing coefficients for the different rovibrational lines observed. In parallel with these measurements, calculations have also been performed on the system at the same three temperatures to obtain theoretical values for the coefficients. The experiments have been carried out using high-resolution stimulated Raman spectroscopy (SRS), while for the calculations two different approaches have been explored: a quantum dynamical calculation and a parametric one utilizing the energy-corrected sudden (ECS) approximation. Comparison between experiment and calculations show good agreement for both the quantum dynamical and the ECS calculated values. This is, to our knowledge, the first reported experimental determination of collisional line broadening and mixing coefficients in the spectrum of N₂ per-

Email address: denis.paredes@iem.cfmac.csic.es (Denís Paredes-Roibás )

turbed by CO. We also present a brief comparison with the results of prior calculations and with measurements conducted not long ago in the reverse collisional system (i.e., CO perturbed by N₂).

Keywords: Collisional Broadening, Line Mixing, Stimulated Raman Spectroscopy, Quantum Dynamical Calculations, N₂-CO

Journal Pre-proof

1 1. Introduction

2 The collisional system formed by the molecules of CO and N₂ has been
3 studied by numerous authors from both the experimental and theoretical
4 points of view. One of the most recent works, in which both experimental and
5 calculated line broadening and mixing coefficients for lines in the Q branch
6 of the Raman spectrum of CO perturbed by N₂ were reported, was carried
7 out by some of us [1]. One common aspect in most of these works –including
8 ours– is that the system has been studied almost exclusively from the point of
9 view of CO as the “active” molecule (i.e., the molecule whose spectrum shows
10 the collisional effects), with N₂ in the role of the perturber species. There
11 are several reasons for this: first and foremost, CO has a permanent dipole
12 moment that allows its detection and study by means of infrared (IR) and
13 microwave (MW) spectroscopies, much more common than the Raman or
14 quadrupole techniques required to record spectra of N₂. This also makes CO
15 a much better candidate for spectroscopic detection and studies in remote
16 environments (e.g., planetary atmospheres or interstellar clouds), since these
17 observations generally rely on IR and MW techniques. Environments in
18 which the presence of both CO and N₂ has been detected in nature include
19 the atmospheres of planetary bodies like Earth, Titan, Pluto and Triton [2–5].
20 Earth’s atmosphere is a prime example of a planetary atmosphere in which
21 CO is present as a trace species while N₂ is present in large concentrations,
22 thus making broadening data of CO perturbed by N₂ very valuable for the
23 correct interpretation of any spectroscopic atmospheric studies involving the
24 molecule of CO.

25 Conversely, there are no experimental and very few theoretical studies
26 of this same collisional pair with N₂ as the perturbed molecule and CO as
27 the perturber (henceforth abbreviated as the N₂-CO system). Besides at-
28 mospheric and astrophysical studies, there are other fields of application in
29 which the availability of accurate N₂-CO line broadening and mixing data
30 would prove valuable. One of these is combustion diagnostics, in which the

31 technique of coherent anti-Stokes Raman spectroscopy (CARS) is commonly
32 used for temperature mapping in flames, engines and jets. This mapping is
33 frequently based on the acquisition and modelling of the Raman spectrum
34 of the N_2 present in combustion mixtures. CO is often present among the
35 combustion products, normally as a minor constituent of the mixture but
36 in concentrations that sometimes may reach a few percent [6] and more. In
37 these cases, incorporating the line broadening and mixing caused by CO in
38 the Raman spectrum of N_2 to the models would improve the accuracy of the
39 temperature results obtained. Afzelius *et al.* investigated this very prob-
40 lem [7] by conducting CARS thermometry experiments and modelizations in
41 mixtures of CO and N_2 and concluded that "... In particular, it is shown
42 that the CO concentration measurement was more accurate if N_2 -CO and
43 CO- N_2 line-broadening coefficients were included in the calculation".

44 From a more fundamental point of view, the availability of N_2 -CO experi-
45 mental broadening and mixing data would make it possible to compare them
46 with the results of different types of calculations, thus allowing the validation
47 of potential energy surfaces (PES) and the evaluation of different calculation
48 methods and approximations.

49 This article presents a joint experimental and theoretical study of the N_2 -
50 CO collisional system, more specifically of the line broadening and mixing in
51 the Q branch of the Raman spectrum of the fundamental vibration ($v = 0 \rightarrow$
52 $v = 1$) of N_2 perturbed by collisions with CO. These are, to our knowledge,
53 the first experimental line broadening and mixing measurements conducted
54 on the N_2 -CO system. Only one prior calculation exists, carried out by
55 Afzelius *et al.* [8] using the semiclassical Robert-Bonamy formalism.

56 The present study has been conducted at three different temperatures and
57 is a natural continuation of our previous work on CO- N_2 in which the roles of
58 the two colliding molecules have been reversed. As such, the techniques and
59 methods used in this work share many aspects with those employed in [1].
60 This is particularly true for the experimental procedures, which are nearly

61 identical to the ones used in that work. For the calculations, different approx-
62 imations not used in [1] have been introduced here. The following sections
63 give a brief overview of the methods, both experimental and theoretical, with
64 emphasis on the main differences between both studies.

65 2. Experimental

66 2.1. Experimental setup

67 All the spectra recorded and analyzed in the course of this work belong to
68 the Q branch ($\Delta j = 0$) of the fundamental vibrational band of N_2 perturbed
69 by collisions with CO. The transitions in this band are forbidden by the elec-
70 tric dipole selection rules but they are accessible by Raman spectroscopy. We
71 used the technique of quasi-continuous stimulated Raman spectroscopy (q-
72 cw SRS) to acquire the high resolution, rotationally resolved spectra required
73 for this study.

74 Our q-cw SRS setup is a two-beam experiment in which the Raman spec-
75 trum is explored by scanning the frequency difference between both laser
76 beams. The Raman signals are then detected as intensity changes in one of
77 the beams, normally denoted “probe beam”. In our setup this is the higher
78 frequency beam, and the Raman signals are detected as intensity losses. This
79 variant of the technique is usually known as stimulated Raman loss (SRL).
80 The experimental setup is nearly identical to the one used in our previous
81 study of the CO- N_2 collisional system [1], so for the sake of brevity we will
82 refer to the different elements of the setup as they appear in the experimen-
83 tal section of that work and highlight only the main differences between that
84 and the present experiment.

85 The cw probe beam is generated by a frequency-stabilized Ar^+ ion laser
86 locked to a hyperfine transition of $^{130}Te_2$ at $18909.44611\text{ cm}^{-1}$. The pulsed
87 pump beam is generated by pulsed optical amplification of a tunable seed
88 provided by a cw dye laser. In order to reach the wavenumber region around
89 2330 cm^{-1} , where the Q branch of the N_2 fundamental lies, the cw dye

90 laser is operated with Rhodamine 590 and the pulsed dye amplifier with
91 Sulforhodamine 640. This allows the generation of pump pulses around \sim
92 16580 cm^{-1} , thus accessing the desired Raman wavenumber difference region.
93 The spectral distribution of the pump pulses, which constitutes the ultimate
94 limit to the instrumental resolution of the apparatus, was measured and can
95 be approximated by a Gaussian function with $\sim 0.0021 \pm 0.0001 \text{ cm}^{-1}$ full
96 width at half maximum (FWHM).

97 The broadening measurements were conducted at three different temper-
98 atures, namely 77, 195 and 298 K. The same sample cell used in Ref. [1] for
99 the 77 and 298 K measurements was used here for the three temperatures.
100 The cooling chamber was left empty for the 298 K measurements and filled
101 with liquid nitrogen for the 77 K measurements. For the 195 K measure-
102 ments the chamber was connected to the forced-flow liquid N_2 evaporation
103 system also described in previous works [9] and the nitrogen evaporation rate
104 adjusted until the desired temperature was reached.

105 We conducted several tests to determine the maximum pulse energy at
106 which the dye amplifier could be operated without inducing additional broad-
107 ening or distortions in the spectral lines due to the alternating current (AC)
108 Stark effect caused by the intense electromagnetic field associated to the laser
109 pulses. The highest safe energy level was determined to be 20 mJ/pulse,
110 which –when our focusing conditions are factored in– equates to a maximum
111 intensity of 162 GW/cm^2 in the focal region. This is a factor of 2 larger
112 than what was measured for the equivalent Q-branch transitions in the CO
113 molecule [1], and is the intensity at which all the present broadening mea-
114 surements have been conducted.

115 One aspect of the measurements that required the introduction of espe-
116 cially tailored modifications to the setup was avoiding the presence of a con-
117 tribution from atmospheric N_2 in the Raman spectra: it is a well known fact
118 that when in an SRS setup the beams are overlapped and travel collinearly
119 a certain distance in open air contributions from atmospheric species, pro-

120 vided that they have Raman-active transitions in the frequency region being
121 probed by the two beams, can be observed in the Raman spectrum. This
122 fact becomes particularly problematic when the species under study inside
123 the cell, typically at a relatively low pressure, is also present in the atmo-
124 sphere: the final result is a compound spectrum in which narrow Raman
125 lines, originating from the sample inside the cell, are riding on top of broader
126 versions of themselves contributed by molecules of the same species present
127 in the atmosphere and thus suffering from significant collisional broadening.
128 N_2 , being the most abundant species in the atmosphere, is the most extreme
129 example of this problem.

130 In order to eliminate the atmospheric N_2 contribution two airtight “vac-
131 uum boxes” were designed, fabricated and incorporated into the setup. They
132 are depicted in Figure 1 together with the sample cell and neighboring opti-
133 cal elements. The role of the boxes is to maintain a vacuum in the zones
134 located immediately before and after the sample cell, where the pump and
135 probe beams are overlapped and travel collinearly. They are made of Plex-
136 iglas (poly methyl methacrylate) and have aluminum bases with threaded
137 holes so that the optics used for beam overlapping, focusing, steering and
138 final beam separation can be installed inside them and kept locked in place.
139 Their overall dimensions are roughly $25 \times 30 \times 35$ cm (width \times length \times height).
140 Both boxes are equipped with uncoated Brewster-angle fused silica windows
141 that match the ones installed on their respective ends of the sample cell. The
142 boxes are placed on the optical bench so that their Brewster windows are in
143 physical contact with the Brewster windows of the cell in order to minimize
144 the distance that the collinear laser beams travel in open air. For the entry
145 of the pump and probe beams into the first box, as well as for the exit from
146 the second box, fused silica windows are installed in the walls of the boxes
147 at perpendicular incidence. The boxes are equipped with capacitive pressure
148 gauges and connected to a rotary pump that is kept in operation for the
149 duration of the measurements. The residual pressure inside the boxes when

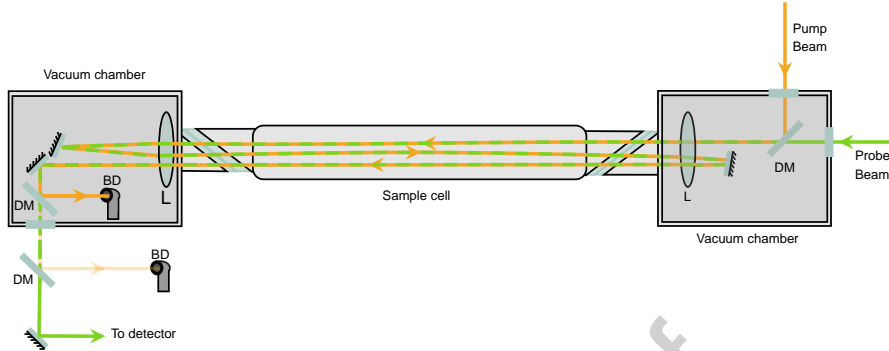


Figure 1: Detail of the sample cell and the vacuum boxes used to remove the contribution of atmospheric N_2 to the Raman spectrum. DM: Dichroic mirror. BD: Beam dump. L: Lens.

150 the pump is in operation is typically ~ 0.1 mbar, which is low enough for the
 151 broad, atmospheric N_2 contribution to completely vanish from the acquired
 152 Raman spectra.

153 Aside from the presence of the vacuum boxes, the only difference with
 154 respect to the optical configuration used in [1] is the use of dichroic mirrors
 155 instead of Pellin-Broca prisms for beam separation. This is done because the
 156 relatively low dispersion of the prisms allowed some partial overlapping of
 157 the two beams as they traveled in air after the second vacuum box before
 158 they were completely separated.

159 The origin and purities of the gases used are the same as in Ref. [1].
 160 N_2 -CO mixtures were prepared *in situ* in the sample cell at room tempera-
 161 ture before each measurement, and cooled afterwards for the measurements
 162 conducted at lower temperatures. A 5% partial pressure of N_2 was used in
 163 the mixtures in all cases. This value represents a compromise that allows
 164 the obtention of acceptable signal-to-noise (S/N) ratios in the spectra while
 165 keeping the effect of N_2 collisional self-broadening sufficiently small for it to
 166 be disregarded: self-broadening coefficients for N_2 - N_2 have values that are
 167 [10] between $\sim 85\%$ (at room temperature) and 91% (at 77 K) of those ob-

168 tained in this work for N₂-CO. At 5% partial pressure this translates into
169 an underestimation of the N₂-CO broadening coefficients that is roughly be-
170 tween 0.45% (at 77 K) and 0.75% (at 298 K) of the obtained values. These
171 errors are well within the uncertainty intervals associated to the coefficients
172 reported in this work.

173 At each one of the three temperatures of reference, spectra of the Q branch
174 of the N₂ fundamental were recorded at five nominal mixture pressures. With
175 some small differences, the pressures selected are essentially the same and
176 cover the same intervals as those in Ref. [1]. Spectra were recorded at least
177 twice at each one of the pressures:

- 178 • At 77 K, total mixture pressures of 5, 15, 30, 45 and 60 mbar were
179 used. Rovibrational lines from Q(0) to Q(10) were recorded under
180 these conditions.
- 181 • At 195 K, total mixture pressures of 10, 25, 50, 80 and 110 mbar were
182 used. Rovibrational lines from Q(0) to Q(14) were recorded.
- 183 • At 298 K, total mixture pressures of 20, 50, 80, 120 and 160 mbar were
184 used. Rovibrational lines from Q(0) to Q(20) were recorded.

185 Although additional, higher rovibrational components were observed (and
186 technically “recorded”) at all temperatures, their S/N ratio was not good
187 enough at all the pressures to allow a sufficiently accurate determination of
188 their collisional line widths.

189 2.2. *Experimental results*

190 Figure 2 presents a view of a section of the Q branch of N₂ perturbed by
191 CO at 77 K and three different total pressures to illustrate the type of spectra
192 recorded in the course of this work. Aside from the absolute wavenumbers,
193 the main visual difference with respect to the previous experiments on the
194 reverse system, CO perturbed by N₂, is the presence of the usual intensity
195 alternation between odd-*j* and even-*j* rotational lines due to the nuclear spin

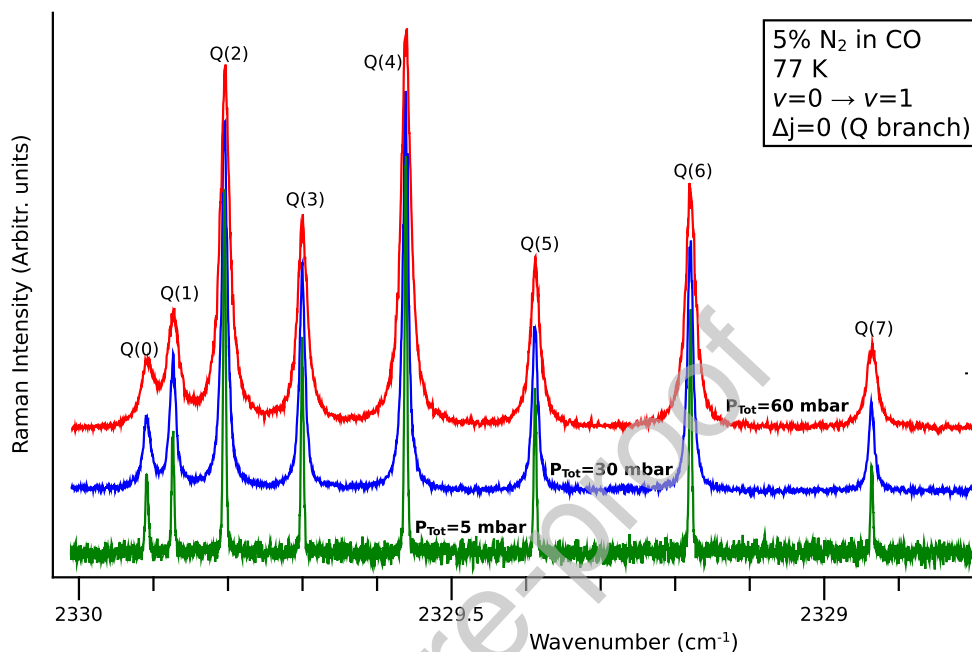


Figure 2: First rovibrational lines of the Q branch of the Raman spectrum of N_2 perturbed by CO registered at 77 K and three different pressures. The three spectra have been normalized using the intensity of the Q(4) line and shifted vertically.

196 statistics of N_2 . The relevance of this alternation lies in that the existence
 197 of ortho and para varieties limits the extent to which line interference (i.e.,
 198 line mixing) is present in the spectrum of N_2 : line interference can only oc-
 199 cur when there are collisionally-mediated transitions between the states of
 200 the interfering lines. Since contiguous lines in the spectrum of N_2 belong to
 201 states of different wavefunction parity, there can be no interference between
 202 them. The only possible line mixing will come from interference between non-
 203 contiguous lines of the same parity (e.g., Q(0), Q(2), Q(4))... and Q(1), Q(3),
 204 Q(5)...), which explains why the effect is subtler than in CO and more dif-
 205 ficult to observe and quantify at the relatively low pressures at which these
 206 experiments have been conducted.

207 Analysis of the spectra was performed using the same procedure employed

208 in [1]: in the absence of velocity-dependent effects (i.e., Dicke narrowing),
209 which we have not observed in our spectra, the basic line shape would be given
210 by the convolution of our apparatus function (Gaussian), Doppler width of
211 the line at the temperature at which the experiment is conducted (Gaussian)
212 and collisional width (Lorentzian), which would yield a Voigt profile with
213 a known Gaussian component. In the presence of line mixing, however,
214 the Lorentzian collisional contribution must be modified. For a case of weak
215 coupling (moderate overlapping of the lines) like the present one Rosenkranz's
216 first order model [11] provides an adequate profile that can be computed as
217 the sum of a Lorentzian and a dispersive function. An expression for the
218 profile is given in Equation A.3 of Appendix A.

219 The Gaussian components of the profiles have FWHMs of 0.0035 cm^{-1}
220 at 77 K, 0.0049 cm^{-1} at 195 K and 0.0058 cm^{-1} at 298 K. Under our experi-
221 mental conditions these values are smaller than the collisional contributions
222 to the widths of the lines except for the lowest pressure series at each tem-
223 perature.

224 We used the same numerical procedure described in [1], which employs a
225 multi-peak fitting algorithm that takes into account the different contribu-
226 tions to the line profiles described above, to extract the Lorentzian collisional
227 widths of the individual rovibrational lines as well as their dispersive con-
228 tributions. For these last ones, the S/N ratio of the spectra and the small
229 magnitude of the interference only allowed a reliable determination for the
230 lines from Q(0) to Q(3) at 77 K. No dispersive contributions have been ob-
231 tained at other temperatures or for other rovibrational lines.

232 The final collisional broadening coefficients γ_j have been determined for
233 each individual rovibrational line Q(j) at each temperature by least squares
234 fitting of a linear function to the collisional widths measured for that line
235 at all the pressures. Each coefficient is obtained from the slope of the fitted
236 function. Additionally, and by fitting the temperature dependence law

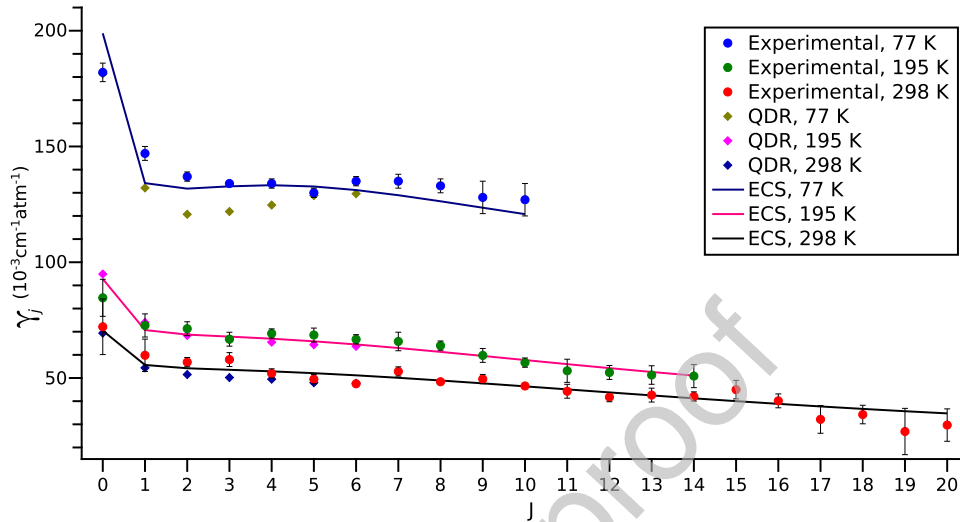


Figure 3: Experimental, Quantum Dynamical Results, QDR, and ECS-calculated broadening coefficients in the Q branch of the Raman spectrum of N_2 perturbed by collisions with CO measured at 77, 195 and 298 K. Error bars in the experimental data represent 1 standard error.

$$\gamma_j(T) = \gamma_j(T_0) \cdot \left(\frac{T_0}{T}\right)^{n_j} \quad (1)$$

237 to the experimental values of our coefficients, we have also determined a
 238 set of n_j exponents. The experimental broadening coefficients are displayed
 239 in Figure 3 together with their calculated values obtained by means of two
 240 different approximations described in the following sections. These sets of
 241 experimental and calculated values are also presented, together with the
 242 experimentally determined n_j exponents, in Table 1.

243 The same linear behavior with pressure of the broadening coefficients
 244 also applies, within the Rosenkranz model, to the Y_j line mixing coefficients.
 245 Their experimentally determined values are presented in Table 2, once again
 246 accompanied by their calculated values.

247 3. Calculations

248 The calculation of collisional line broadening and mixing coefficients re-
249 quires the obtention of a relaxation matrix W (see Appendix A), whose
250 elements can in turn be obtained from the state-to-state collisional rates for
251 the system. Collisional rates are derived from thermally averaged bistate to
252 bistate cross sections. If an intermolecular potential energy surface (PES) is
253 available for the system, accurate calculation of these cross-sections is possi-
254 ble, but computationally expensive. The most accurate method to determine
255 the cross sections, the close coupling (CC) method, is very time consuming
256 to the point of making the problem intractable when the kinetic energy be-
257 comes too large (see the discussions in Refs. [1, 12]). Therefore, in this
258 work we have resorted to two approximate methods. One of them is the use
259 of the infinite order sudden approximation (IOSA), which relies on several
260 quantum approximations, to supplement the full dynamical CC calculation
261 at high kinetic energies. The other one is the energy-corrected sudden ap-
262 proximation, which instead of solving the dynamical calculation relies on the
263 use of a parametric model to describe the elements of the relaxation matrix.
264 Both approaches and their application to our system are briefly discussed in
265 the following sections.

266 3.1. Dynamical calculations

267 In Ref. [1] we performed quantum dynamical calculations on the CO-N₂
268 potential energy surface (PES) of Liu *et al.* [13]. As shown in [1] and [12] this
269 PES is accurate enough for producing pressure broadening coefficients. For
270 the present work we have completed these calculations up to a total energy of
271 $\sim 500 \text{ cm}^{-1}$ using the close-coupling method¹ and by additional calculations
272 at 600, 700 and 800 cm^{-1} using the IOS approximation as implemented in the
273 MOLSCAT code [14]. Our previous work [1] was devoted to CO perturbed by

¹In order to perform CC calculations between 315 and 500 cm^{-1} we used a varying step for the total angular momentum J from 2 to 4.

274 N₂. Rovibrational quantum numbers with subscripts 1 and 2 were associated
 275 with CO and N₂ respectively, in particular for the bistate to bistate kinetic
 276 energy dependent cross sections, $\sigma(j_1 j_2 \rightarrow j'_1 j'_2; E_{kin})$. Since the PES is the
 277 same for the present study we just have to affix subscripts 1 and 2 to the
 278 N₂ and CO molecules. The CO molecule is in its ground vibrational state
 279 while the N₂ molecule can be either in its ground or first excited vibrational
 280 states. However, because the N₂ molecule is quite rigid owing to its triple
 281 bond, the N₂-CO PES depends only weakly on the N₂ vibrational state, thus
 282 scattering calculations consider both molecules in their ground state. We
 283 therefore disregard any vibrational effects.

284 Since the MOLSCAT code provides us bistate-to-bistate cross sections at
 285 various kinetic energies we first introduce a partial pressure broadening cross
 286 section as:

$$\sigma_{ppb}(j_1, j_2; E_{kin}) = \sum_{j'_1 \neq j_1} \sum_{j'_2} \sigma(j_1 j_2 \rightarrow j'_1 j'_2; E_{kin}). \quad (2)$$

287 As in [1] we first extrapolate the bistate-to-bistate cross sections up to 2000
 288 cm⁻¹ and then perform a thermal average at a given temperature T over the
 289 kinetic energy distribution to obtain a partial pressure broadening coefficient:

$$\gamma_{ppb}(j_1, j_2; T) = \sum_{j'_1 \neq j_1} \sum_{j'_2} R(j_1 j_2 \rightarrow j'_1 j'_2; T). \quad (3)$$

290 where $R(j_1 j_2 \rightarrow j'_1 j'_2; T)$ is a bistate-to-bistate collisional rate. Finally, the
 291 (total) pressure broadening coefficient of a $Q(j_1)$ line is given by:

$$\gamma(j_1; T) = \sum_{j_2} \rho(j_2) \gamma_{ppb}(j_1, j_2; T). \quad (4)$$

292 The reader can compare the derivation of Eq. (4) with equations (A.1) and
 293 (A.2). Because our calculations are not reliable for high rotational quantum
 294 numbers (too few points) or bistate to bistate cross sections are not available

295 (more precisely when the rotational energy $E_{j_1 j_2}$ exceeds $\sim 300 \text{ cm}^{-1}$) we
 296 assumed that the partial pressure broadening coefficient for $j_2 > 7$ can be
 297 deduced from the ones for $j_2 \leq 7$. This approximation has been successfully
 298 applied before for many interacting pairs [1, 9, 10, 12, 15–18].

299 In the following we call the results obtained with this method the QDR
 300 set for quantum dynamical results. Pressure broadening coefficients derived
 301 from this set are given in Table 1. Due to the various approximations done, a
 302 limited grid in energy, the use of the IOSA, a polynomial extrapolation of the
 303 bistate cross sections, the extrapolation of the partial pressure broadening
 304 rates for $j_2 > 7$, we do not expect our results to be accurate by more than
 305 10% at room T . At 195 K we estimate our results to be accurate within
 306 about 5% and to a few percents at 77 K.

307 3.2. Parametric calculations

We now briefly describe the alternative semi-empirical method we have used. This method is based on the Infinite Order Sudden Approximation (IOSA). The IOSA allows a separation of angular couplings and dynamics. It has been thoroughly discussed in the literature ([19–21]). Within the IOSA bistate rate constants are derived from thermally averaged, over the Maxwell-Boltzmann kinetic energy distribution at a temperature T , downward inelastic cross sections to the ground state $j_1 = j_2 = 0$:

$$\begin{aligned}
 R(j_1 j_2 \rightarrow j'_1 j'_2) &= (2j'_1 + 1)(2j'_2 + 1) \\
 &\times \sum_{L_1 L_2} (2L_1 + 1)(2L_2 + 1) \begin{pmatrix} j_1 & L_1 & j'_1 \\ 0 & 0 & 0 \end{pmatrix}^2 \begin{pmatrix} j_2 & L_2 & j'_2 \\ 0 & 0 & 0 \end{pmatrix}^2 \\
 &\times R(L_1 L_2 \rightarrow 00) \quad (5)
 \end{aligned}$$

308 Because the IOS approximation ignores the rotational energy spacings (i.e.
 309 the IOS invokes the energy sudden approximation) there is no difference
 310 between the total energy and the kinetic energy. As a consequence, the

311 detailed balance principle is not satisfied. Following DePristo *et al.* [22] Eq.
 312 (5) is used for deexcitation transitions (i.e. those for which $E_{j_1 j_2} \geq E_{j'_1 j'_2}$)
 313 while upward rates are obtained by imposing the detailed balance.

Off-diagonal relaxation matrix elements are then given by [19]:

$$W(j'_1, j_1) = -(2j'_1 + 1) \sum_{L_1} (2L_1 + 1) \begin{pmatrix} j_1 & L_1 & j'_1 \\ 0 & 0 & 0 \end{pmatrix}^2 \tilde{R}(L_1 \rightarrow 0), \quad (6)$$

314 with the help of an effective one body rate:

$$\tilde{R}(L_1 \rightarrow 0) = \sum_{L_2} (2L_2 + 1) R(L_1 L_2 \rightarrow 00). \quad (7)$$

In order to correct for the energy defect of the IOS method, or that the molecules do rotate during a collision, DePristo *et al.* [22] introduced the Energy Corrected Sudden (ECS) method. Corrected downward rates are expressed through:

$$\begin{aligned} R(j_1 j_2 \rightarrow j'_1 j'_2) &= (2j'_1 + 1)(2j'_2 + 1) \\ &\times \sum_{L_1 L_2} (2L_1 + 1)(2L_2 + 1) \begin{pmatrix} j_1 & L_1 & j'_1 \\ 0 & 0 & 0 \end{pmatrix}^2 \begin{pmatrix} j_2 & L_2 & j'_2 \\ 0 & 0 & 0 \end{pmatrix}^2 \\ &\times A(j_1 j_2; L_1 L_2)^2 R(L_1 L_2 \rightarrow 00), \quad (8) \end{aligned}$$

where at this point we are not concerned about the "exact" expression of the adiabaticity factor A . Again, excitation rates are calculated by invoking detailed balancing. Starting from Eq. (8) it is not possible to derive an equation similar to Eq. (6) because of the dependence of the adiabaticity factor with the rotational quantum number j_2 . Following many previous works dealing with diatom-diatom systems [23–26], we assume that Eq. (6)

is transposable to the ECSA:

$$W(j', j) = -\frac{\rho_{j>}}{\rho_j} (2j_{<} + 1) \sum_{L \neq 0} (2L + 1) A(j_{>}; L)^2 Q'_L(T) \quad (9)$$

315 where the subscripts “1” have been dropped since this is the standard ECS
 316 expression for a diatom-atom system. The $Q'_L(T)$ are effective one-rotor rate
 317 constants from level L to the level $j = 0$ at a given T , also called in the
 318 literature the basic rates. The detailed balance, $\rho(j)W(j', j) = \rho(j')W(j, j')$,
 319 has been enforced in Eq. (9) since $j_{>} (j_{<})$ stands for the larger (resp. smaller)
 320 value of (j, j') . The adiabaticity factors write:

$$A(j_{>}; L) = \sqrt{\frac{\Omega_{j_{>}}}{\Omega_L}}, \quad (10)$$

321 where for the Ω 's we have used the form proposed by Bonamy *et al.* [27]:

$$\Omega_j = \left[1 + \frac{1}{12} (\omega_{j,j-2} \tau_c)^2 \right]^{-1}. \quad (11)$$

322 $\hbar\omega_{j,j-2}$ is the energy difference between the level j and the next lower acces-
 323 sible one ($j - 2$ because of the ortho-para species of N_2). τ_c is the effective
 324 duration of a collision that may be expressed in term of the scaling length ℓ_c
 325 since $\ell_c = \bar{v}_r \tau_c$, with \bar{v}_r the mean relative speed at T . Setting $\ell_c = 0$ returns
 326 the IOSA for a diatom-atom system.

327 In conjunction with the ECSA, the basic rates were modeled using a
 328 simple power law [23, 26]:

$$Q'_L(T) = \frac{A(T)}{[L(L+1)]^\alpha}. \quad (12)$$

329 In addition, similarly to the usual power law for the pressure broadening co-
 330 efficient, the temperature dependent scaling parameter $A(T)$ can be written

331 [23]:

$$A(T) = A(T_0) \left(\frac{T_0}{T} \right)^N \quad (13)$$

332 where T_0 is a reference temperature (296 K in our case). Therefore our fitting
 333 parameters are $A(T_0)$, N , the exponent α and the scaling length ℓ_c .

334 We first performed a global nonlinear fit of the four parameters to the
 335 whole set of experimental values at all temperatures, and obtained $\alpha = 0.94$,
 336 $\ell_c = 1.2 \text{ \AA}$, $N = 1.2$ and $A(T_0) = 34.3 \cdot 10^{-3} \text{ cm}^{-1} \text{ atm}^{-1}$. Since in this kind of
 337 problem there is always going to be a certain correlation between the fitted
 338 values, we explored an alternative approach based on performing a sequence
 339 of more restricted fits: firstly, for each temperature we fitted a system with
 340 α , ℓ_c and $A(T)$ as free parameters, obtaining $\alpha = 0.93$ and $\ell_c = 1.08 \text{ \AA}$ at 77
 341 K, $\alpha = 1.03$ and $\ell_c = 1.01 \text{ \AA}$ at 195 K, and $\alpha = 1.13$ and $\ell_c = 0.94 \text{ \AA}$ at 298
 342 K; associated $A(T)$ values are not reported. Averaging the values of α and
 343 ℓ_c at the three temperatures one obtains $\alpha = 1.03$ and $\ell_c = 1.01 \text{ \AA}$, which we
 344 adopt as temperature-independent values for these parameters. With these
 345 two fixed, one can fit again the expressions to the experimental data at each
 346 one of the three temperatures to obtain fitted values for $A(T)$, which turn
 347 out to be $A(77K) = 220.23$, $A(195K) = 71.02$ and $A(298K) = 47.25$ in 10^{-3}
 348 $\text{cm}^{-1} \text{ atm}^{-1}$. Finally, fitting for $\ln A(T)$, with $A(T)$ given by Eq. (13), leads
 349 to an exponent $N = 1.15$ and $A(T_0) = 46.06 \cdot 10^{-3} \text{ cm}^{-1} \text{ atm}^{-1}$. The final set
 350 of parameters obtained through this sequential procedure is thus $\alpha = 1.03$,
 351 $\ell_c = 1.01 \text{ \AA}$, $N = 1.15$ and $A(T_0) = 46.06 \cdot 10^{-3} \text{ cm}^{-1} \text{ atm}^{-1}$. With the
 352 exception of $A(T_0)$, these values are close to the ones obtained by means of
 353 the global four-parameter fit.

354 The values obtained for the broadening coefficients using the parameters
 355 issued from this sequential fit are reported on Fig. 3 and Table 2. Overall,
 356 they compare well with the values deduced from the experimental measure-
 357 ments.

358 Figure 4 compares the fitted ECS basic rates, $Q'(L; T)$, with the effec-
 359 tive rates, $\tilde{R}(L \rightarrow 0; T)$, coming from our quantum dynamical calculations

j	γ_j						n_j			
	77 K		195 K		298 K					
	Exp.	QDR	ECS	Exp.	QDR	ECS	Exp.	QDR	ECS	Exp.
0	182(4)	181.5	198.9	85(8)	94.9	92.8	72(12)	69.4	70.5	0.75(7)
1	147(3)	132.1	134.2	73(5)	74.0	70.7	60(7)	54.4	55.6	0.71(5)
2	137(2)	120.7	131.8	71(3)	68.4	68.7	57(2)	51.5	54.2	0.66(3)
3	134(1)	121.9	132.8	67(3)	66.5	67.9	58(3)	50.2	53.6	0.65(6)
4	134(2)	124.7	133.3	69(2)	65.5	67.0	52(2)	49.5	52.9	0.70(2)
5	130(2)	128.8	132.7	69(3)	64.4	65.9	49(2)	48.0	52.1	0.71(3)
6	135(2)	129.6	131.2	67(2)	63.7	64.5	48(1)	47.7	51.2	0.77(2)
7	135(3)		129.0	66(4)		63.0	53(2)		50.1	0.70(4)
8	133(3)		126.3	64(2)		61.3	48(1)		48.9	0.75(3)
9	128(7)		123.6	60(3)		59.5	50(2)		47.7	0.71(7)
10	127(7)		120.8	57(2)		57.8	47(1)		46.4	0.73(9)
11				53(5)		56.0	44(3)		45.1	
12				52(3)		54.3	42(2)		43.8	
13				51(4)		52.6	43(3)		42.5	
14				51(5)		51.0	42(2)		41.2	
15							45(4)		40	
16							40(3)		38.8	
17							32(6)		37.7	
18							34(4)		36.7	
19							27(10)		35.7	
20							30(7)		34.7	

Table 1: Experimental (Exp.) and calculated (QDR and ECS) values of the collisional broadening coefficients for the lines of the Q branch of the Raman spectrum of N_2 perturbed by CO at 77, 195 and 298 K, and experimentally determined temperature dependence exponents n_j . Broadening coefficients are given in units of $10^{-3} \cdot \text{cm}^{-1} \cdot \text{atm}^{-1}$. Numbers in parentheses are in units of the last digit of the main value they refer to and represent 1 standard error.

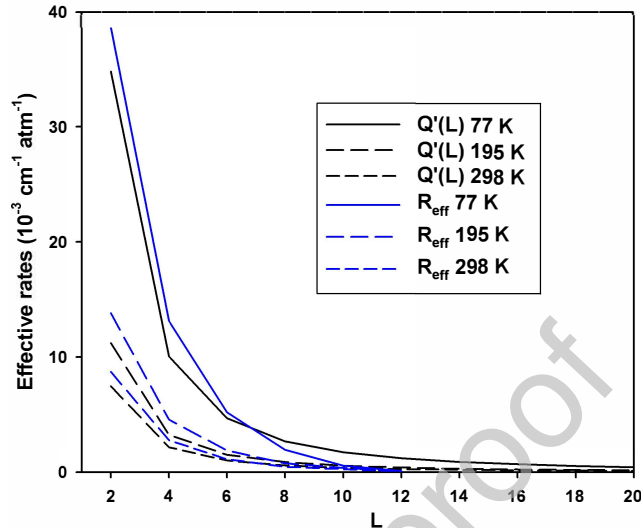


Figure 4: Comparison of effective one body rates. The $Q'(L;T)$ are obtained from the ECS $A(T)$ fit and R_{eff} designates $\tilde{R}(L \rightarrow 0;T)$ as given by Eq. (7) and derived from our QDR set.

(Sec. 3.1). This comparison is surprisingly good, justifying *a posteriori* the
 360 diatom-atom ECS method used in the present study and in many works in
 361 which fitted one body basic rates were used, without any support of dynam-
 362 ical calculations, to model pressure broadening and line mixing coefficients
 363 [24–26, 28].
 364

365 Finally, the line mixing parameters, Eq. (A.4) can be evaluated starting
 366 with the basic rates or our QDR set. Table 2 gathers our results and compare
 367 them with our experimental values.

368 4. Discussion

369 The first conclusion that can be extracted from Figure 3 is that QDR
 370 calculations are able to reproduce the experimental data with reasonable
 371 accuracy. In fact the agreement is quite good at 195 and 298 K, while at
 372 77 K the calculations underestimate the experimental coefficients by $\sim 10\%$
 373 between $j = 1$ and $j = 4$. This deviation is larger than initially expected, but

j	Y_j^P						
	77 K			195 K		298 K	
	Exp.	QDR	ECS	QDR	ECS	QDR	ECS
0	-1.9(2)	-2.35	-2.95	-1.00	-1.15	-0.66	-0.80
1	-1.2(2)	-1.15	-1.26	-0.50	-0.55	-0.32	-0.40
2	-0.18(6)	-0.13	-0.01	-0.13	-0.12	-0.09	-0.11
3	0.2(1)	0.24	0.30	0.00	0.00	-0.01	-0.02
4		0.35	0.38	0.04	0.05	0.01	0.01
5		0.37	0.38	0.05	0.06	0.01	0.02
6		0.35	0.35	0.06	0.07	0.02	0.03
7		0.33	0.31	0.07	0.07	0.03	0.03

Table 2: Experimental (Exp.) and calculated (QDR and ECS) Rosenkranz line mixing coefficients Y_j^P for the first $Q(j)$ lines in the fundamental band of the Raman spectrum of N_2 perturbed by CO at 77, 195 and 298 K. Units are atm^{-1} . Numbers in parentheses are given in units of the last digit of the main value they refer to and represent 1 standard error.

374 not unusually so: in fact, a very similar discrepancy between experiment and
375 calculations, in this case performed using a combination of the close coupling
376 and coupled states (CS) methods instead of CC+IOSA, was observed in the
377 reverse CO- N_2 system at 77 K. Figure 7 in Ref. [1] illustrates these differences
378 which are, like those in the present work, especially noticeable for the lines
379 between $j = 1$ and $j = 4$ at 77 K and have magnitudes of $\sim 10\%$ of the
380 experimental value.

381 The calculations based on the ECS approximation are able to reproduce
382 the experimental data satisfactorily. The fact that the measurements are
383 well reproduced for the whole range of rovibrational components and at the
384 three temperatures with fixed (pre-fitted) values for α and l_c , by just fitting
385 the temperature dependence of the scaling parameter $A(T)$, indicates that
386 the ECS model is indeed able to provide reasonably accurate values for the

387 elements of the relaxation matrix in this system.

388 Both approximations seem to be able to reproduce the line mixing coef-
389 ficients at 77 K with the exception of the first one Y_0^p , but the small size of
390 the experimental data set and the large uncertainties associated to the values
391 limits the usefulness of this comparison.

392 As for how our results compare to those obtained by other authors, the
393 only available data set is the one obtained by Afzelius *et al.* [8] by means of
394 semiclassical Robert-Bonamy (RB) calculations at 295 and 1000 K. N₂-CO
395 broadening coefficients are displayed in Figure 7 of their article with no ac-
396 companying numerical values: at 295 K, and starting at $\sim 0.070 \text{ cm}^{-1}\cdot\text{atm}^{-1}$
397 for Q(0), the value of the coefficient drops sharply for Q(1) and then decreases
398 smoothly and slowly for increasing values of j , reaching $\sim 0.045 \text{ cm}^{-1}\cdot\text{atm}^{-1}$
399 around Q(14). Aside from a small dip around Q(1) that is not clearly visible
400 in our data, both the magnitude and overall tendency and rate of change of
401 their broadening coefficients look similar to those in our experimental data.
402 No deeper conclusions can be extracted without access to the numerical data.

403 Finally, it is interesting to compare our N₂-CO broadening coefficients
404 with the ones we obtained in our previous work for the reverse system, CO-
405 N₂, since the molecular interaction is governed by the same intermolecular
406 forces. Figure 5 shows this comparison using our CO-N₂ bibliographic data
407 [1]. Disregarding extreme points, which are affected by larger errors, it is
408 evident that the general behavior of the coefficients and their j dependence is
409 the same for both systems at the three temperatures, with the main difference
410 being the magnitudes of the coefficients themselves: N₂-induced broadenings
411 in the spectrum of CO are $\sim 20\%$ larger than CO-induced broadenings in
412 the spectrum of N₂ at the three temperatures. This may result surprising
413 at first glance considering the similarities between the two molecules: they
414 are isoelectronic, have the same mass, very similar rotational constants (B_e
415 in the ground electronic state is $\sim 3.5\%$ larger for N₂ than for CO) and only
416 slightly ($\sim 10\%$) different vibrational frequencies. CO has a permanent dipole

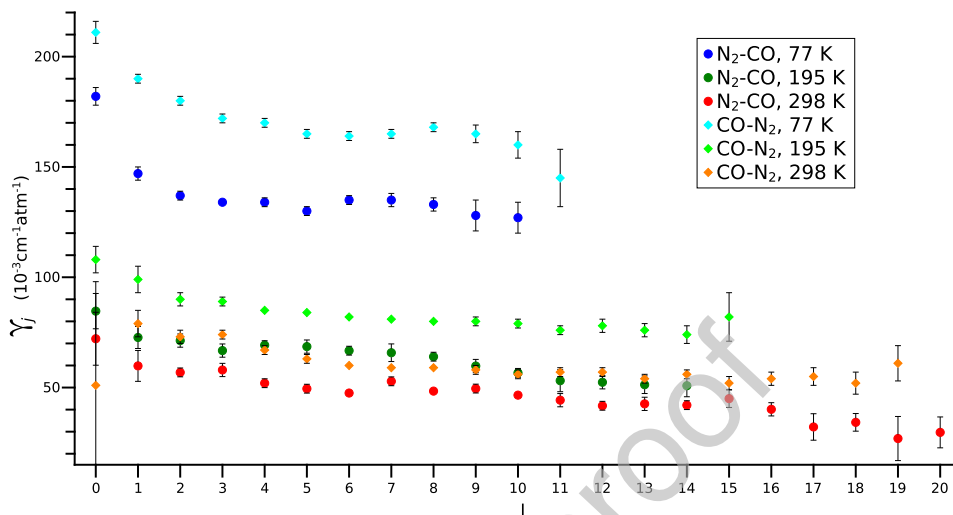


Figure 5: Comparison of Raman Q-branch experimental broadening coefficients for the $\text{N}_2\text{-CO}$ system (this work) and the CO-N_2 system (taken from [1]) at 77, 195 and 298 K. Error bars in the experimental data represent 1 standard error.

417 moment but it is rather small (~ 0.1 D), so it can be considered an “almost
418 homonuclear” molecule.

419 In order to understand the difference in the magnitude of the broaden-
420 ing coefficients for these two systems, it is helpful to look first at the values
421 of these same coefficients for the CO-CO and $\text{N}_2\text{-N}_2$ self-perturbed pairs.
422 Looney and Rosasco [29] performed RB calculations on these systems, which
423 were later revisited by Afzelius *et al.* [8]. The results, which used potential
424 energy surfaces with parameters adjusted to better reproduce the experi-
425 mental data already available for the systems, are presented in Figure 7 of
426 Afzelius’ article: at 295 K, the broadening coefficients in the Q branch of the
427 Raman spectrum are considerably larger ($\sim 50\%$) for CO-CO than for $\text{N}_2\text{-N}_2$.
428 More importantly, the authors identified the quadrupole-quadrupole symme-
429 try interaction in the PES as the dominant one in both systems: according to
430 their calculations, the dipole-dipole and dipole quadrupole interactions only
431 account for less than $\sim 10\%$ of the pressure broadening coefficients in low and

432 intermediate $Q(j)$ lines ($j \leq 12$) in the CO-CO collisional system, and up to
433 20% for $j = 18$ [29]. Since the electronic quadrupole moment of CO is larger
434 than that of N_2 (-1.9×10^{-26} esu vs. -1.4×10^{-26} esu), this fact by itself
435 would be enough to explain the larger broadening coefficients of CO vs. N_2
436 in the case of self collisions. Following the same line of reasoning, one would
437 also expect the same quadrupole-quadrupole term to dominate the interac-
438 tion between a molecule of CO and a molecule of N_2 , and thus the broadening
439 coefficients of the CO- N_2 and N_2 -CO systems should show values that are in
440 between those of the two self-perturbed systems. Indeed, broadening coeffi-
441 cients calculated for the heteromolecular pairs are also presented in the same
442 aforementioned figure and clearly show that the overall magnitude of the
443 coefficients follows the sequence $CO-CO > CO-N_2 > N_2-CO > N_2-N_2$, matching
444 our experimental results for the two intermediate systems. Notice, however,
445 that the quadrupole-quadrupole interaction argument applies equally to CO-
446 N_2 and to N_2 -CO, since the collision is the same for both systems, and thus
447 it does not explain the difference observed between them.

448 The key element to the different behavior of the two heteromolecular
449 systems seems to lie in the restriction imposed to the molecule of N_2 by the
450 symmetry of its nuclear wavefunction (i.e., the existence of ortho and para
451 N_2 species): if as a consequence of a collision a molecule of N_2 changes its
452 rotational state it will have to obey the rule $\Delta j = \pm 2, \pm 4, \dots$ to preserve
453 the symmetry of the wavefunction. Thus, transitions that follow the dipole
454 selection rule $\Delta j = \pm 1$ as a consequence of a collision are forbidden for N_2 ,
455 but allowed for CO, which is not bound by the same symmetry restriction.
456 As stated above the dominant interaction in a collision between a molecule
457 of CO and a molecule of N_2 is described by the quadrupole-quadrupole term,
458 which will only induce $\Delta j = \pm 2$ transitions, but interactions like the dipole-
459 quadrupole or dipole-spherical coupling terms, although smaller, do exist
460 and will give rise to additional $\Delta j = \pm 1$ and other transitions that are only
461 allowed for the molecule of CO. To summarize, when a CO molecule in a given

462 rotational state j and a molecule of N_2 in j' collide the CO molecule has a
 463 larger number of accessible channels leading to other rotational states than
 464 the N_2 molecule, and some of these channels ($\Delta j = \pm 1$) involve a smaller
 465 energy gap than the ones accessible to N_2 . The end result is that in a collision
 466 between a CO and an N_2 molecule the overall probability of experiencing a
 467 rotationally inelastic collision is higher for CO than it is for N_2 , leading to
 468 larger collisional broadening coefficients for CO- N_2 than for N_2 -CO.

469 Acknowledgments

470 DPR and RZM acknowledge the funding received from Ministerio de Cien-
 471 cia e Innovación through Project PID2021-123752NB-I00. We also thank
 472 Luis de Prado for his skillful fabrication of the vacuum boxes.

473 Appendix A. Relaxation matrix elements and line coupling coef- 474 ficients

475 In the following we denote an isotropic Raman transition from an initial
 476 state j_1 to a final one having the same rotational quantum number j_1 by the
 477 line $|j_1 j_1\rangle\rangle$. In this case an off-diagonal relaxation matrix element, coupling
 478 this line with another one defined by j'_1 ($j'_1 \neq j_1$), is nothing but minus a
 479 weighted summation of rate constants [19]:

$$\langle\langle j'_1 j'_1 | W | j_1 j_1 \rangle\rangle \equiv W(j'_1, j_1) = - \sum_{j_2} \rho(j_2) \sum_{j'_2} R(j_1 j_2 \rightarrow j'_1 j'_2), \quad (\text{A.1})$$

480 where the ρ 's are the population of the perturbing molecule at a given tem-
 481 perature T . A diagonal term, representing the collisional half width at half
 482 maximum (HWHM) of a Lorentzian line profile, is in turn given by the (ex-
 483 act) sum rule:

$$W(j_1, j_1) = - \sum_{j'_1 \neq j_1} W(j'_1, j_1) \quad (\text{A.2})$$

484 A simple profile which takes into account the coupling between the lines
 485 forming a band is the Rosenkranz [11] profile:

$$I(\omega) = \sum_j S_j \frac{\Gamma_j + Y_j (\omega - \omega_j)}{(\omega - \omega_j)^2 + \Gamma_j^2} \quad (\text{A.3})$$

486 where we ignore the shift in our rigid rotators approximation. In Eq. (A.3)
 487 ω is the pulsation of observation, S_j are the line intensities, ω_j are the central
 488 frequencies of the unperturbed lines, Γ_j are the collisional HWHM, $W(j, j)$,
 489 and finally Y_j are the first order, in pressure, line mixing coefficients. The
 490 latter are given by:

$$Y_j = 2 \sum_{j' \neq j} \frac{W(j', j)}{\omega_j - \omega_{j'}}. \quad (\text{A.4})$$

491 **References**

- 492 [1] D. Paredes-Roibás, R. Z. Martínez, H. Józwiak, F. Thibault, Collisional
493 line broadening and mixing in the Raman spectrum of CO perturbed by
494 N₂: Experimental measurements and theoretical calculations, *Journal*
495 *of Quantitative Spectroscopy and Radiative Transfer* 275 (2021) 107868.
- 496 [2] N. D. Sze, Anthropogenic CO emissions: Implications for the atmo-
497 spheric CO-OH-CH₄ cycle, *Science* 195 (1977) 673–675.
- 498 [3] B. L. Lutz, C. De Bergh, T. Owen, Titan: Discovery of carbon monoxide
499 in its atmosphere, *Science* 220 (1983) 1374–1375.
- 500 [4] T. C. Owen, T. L. Roush, D. P. Cruikshank, J. L. Elliot, L. A.
501 Young, C. De Bergh, B. Schmitt, T. R. Geballe, R. H. Brown, M. J.
502 Bartholomew, Surface ices and the atmospheric composition of pluto,
503 *Science* 261 (1993) 745–748.
- 504 [5] D. P. Cruikshank, T. L. Roush, T. C. Owen, T. R. Geballe, C. De Bergh,
505 B. Schmitt, R. H. Brown, M. J. Bartholomew, Ices on the surface of
506 Triton, *Science* 261 (1993) 742–745.
- 507 [6] D. Klick, K. A. Marko, L. Rimai, Broadband single-pulse cars spectra
508 in a fired internal combustion engine, *Appl. Opt.* 20 (1981) 1178–1181.
- 509 [7] M. Afzelius, C. Brackmann, F. Vestin, P.-E. Bengtsson, Pure rotational
510 coherent anti-Stokes Raman spectroscopy in mixtures of CO and N₂,
511 *Appl. Opt.* 43 (2004) 6664–6672.
- 512 [8] M. Afzelius, P.-E. Bengtsson, J. Bonamy, Semiclassical calculations of
513 collision line broadening in Raman spectra of N₂ and CO mixtures, *J.*
514 *Chem. Phys.* 120 (2004) 8616–8623.
- 515 [9] F. Thibault, B. Corretja, A. Viel, D. Bermejo, R. Z. Martínez,
516 B. Busseroy-Honvault, Linewidths of C₂H₂ perturbed by H₂: experiments

- 517 and calculations from an *ab initio* potential, Phys. Chem. Chem. Phys.
518 10 (2008) 5419–5428.
- 519 [10] F. Thibault, R. Z. Martínez, D. Bermejo, L. Gómez, Collisional line
520 widths of autoperturbed N₂: Measurements and quantum calculations,
521 J. Quant. Spectrosc. Radiat. Transf 112 (2011) 2542–2551.
- 522 [11] P. W. Rosenkranz, Shape of the 5 mm Oxygen Band in the Atmosphere,
523 IEEE Transactions on Antennas and Propagation AP-23 (1975) 498–
524 506.
- 525 [12] H. Józwiak, F. Thibault, H. Cybulski, P. Wcisło, Ab initio investigation
526 of the CO-N₂ quantum scattering: the collisional perturbation of the
527 pure rotational R(0) line in CO, The Journal of Chemical Physics 154
528 (2021) 054314.
- 529 [13] J.-M. Liu, Y. Zhai, X.-L. Zhang, H. Li, Intermolecular configurations
530 dominated by quadrupole-quadrupole electrostatic interactions: explicit
531 correlation treatment of the five-dimensional potential energy surface
532 and infrared spectra for the CO-N₂ complex, Phys. Chem. Chem. Phys.
533 20 (2018) 2036–2047.
- 534 [14] J. M. Hutson, C. R. Le Sueur, MOLSCAT: A program for non-reactive
535 quantum scattering calculations on atomic and molecular collisions,
536 Computer Physics Communications 241 (2019) 9–18.
- 537 [15] L. Gomez, R. Z. Martínez, D. Bermejo, F. Thibault, P. Joubert,
538 B. Bussery-Honvault, J. Bonamy, Q-branch linewidths of N₂ perturbed
539 by H₂: Experiments and quantum calculations from an *ab initio* poten-
540 tial, J. Chem. Phys. 126 (2007) 204302.
- 541 [16] F. Thibault, E. Fuller, K. Grabow, J. Hardwick, C. Marcus, D. Marston,
542 L. Robertson, E. Senning, M. Stoffel, R. Wiser, Experimental line broad-
543 ening and line shift coefficients of the acetylene $\nu_1 + \nu_3$ band pressurized

- 544 by hydrogen and deuterium and comparison with calculations, *J. Mol.*
545 *Spectrosc* 256 (2009) 17–27.
- 546 [17] F. Thibault, R. Z. Martínez, D. Bermejo, S. V. Ivanov, O. G. Buzykin,
547 Q. Ma, An experimental and theoretical study of nitrogen-broadened
548 acetylene lines, *J. Quant. Spectrosc. Radiat. Transf* 142 (2014) 17–24.
- 549 [18] A. Zadrożny, H. Józwiak, E. Quintas-Sánchez, R. Dawes, P. Wcisło, Ab
550 initio quantum scattering calculations for the CO–O₂ system and a new
551 CO–O₂ potential energy surface: O₂ and air broadening of the R(0) line
552 in CO, *The Journal of Chemical Physics* 157 (2022) 174310.
- 553 [19] S. Green, Raman linewidths and rotationally inelastic collision rates in
554 nitrogen, *J. Chem. Phys.* 98 (1993) 257–268.
- 555 [20] D. J. Kouri, in *Atom-molecule Collision Theory; a Guide for the Exper-*
556 *imentalist*, Ed R.B. Bernstein, Plenum, 1979.
- 557 [21] A. E. DePristo, H. Rabitz, The collision of two linear rotors: A scaling
558 theoretical analysis of the H₂–H₂ and HF–HF systems, *The Journal of*
559 *Chemical Physics* 72 (1980) 4685–4692.
- 560 [22] A. E. DePristo, S. D. Augustin, R. Ramaswamy, H. Rabitz, Quantum
561 number and energy scaling for nonreactive collisions, *J. Chem. Phys.* 71
562 (1979) 850–865.
- 563 [23] G. Millot, Rotationally inelastic rates over a wide temperature range
564 based on an energy corrected sudden–exponentialpower theoretical anal-
565 ysis of Raman line broadening coefficients and Q branch collapse, *J.*
566 *Chem. Phys.* 93 (1990) 8001–8010.
- 567 [24] J.-P. Bouanich, R. Rodrigues, C. Boulet, Line mixing effects in the 1
568 $\leftarrow 0$ and 2 $\leftarrow 0$ CO bands perturbed by CO and N₂ from low to high
569 densities, *Journal of Quantitative Spectroscopy and Radiative Transfer*
570 54 (1995) 683–693.

- 571 [25] A. Predoi-Cross, J. P. Bouanich, D. C. Benner, A. D. May, J. R. Drum-
572 mond, Broadening, shifting, and line asymmetries in the $2\leftarrow 0$ band of
573 CO and CO-N₂: Experimental results and theoretical calculations, *J.*
574 *Chem. Phys.* 113 (2000) 158–168.
- 575 [26] J.-M. Hartmann, C. Boulet, D. Robert (Eds.), *Collisional Effects on*
576 *Molecular Spectra* (Second Edition), Elsevier, Amsterdam, 2021.
- 577 [27] L. Bonamy, J. M. Thuet, J. Bonamy, D. Robert, Local scaling analysis
578 of state-to-state rotational energy transfer rates in N₂ from direct mea-
579 surements, *J. Chem. Phys.* 95 (1991) 3361–3370.
- 580 [28] F. A. Bendana, D. D. Lee, C. Wei, D. I. Pineda, R. M. Spearrin, Line
581 mixing and broadening in the $v(1\rightarrow 3)$ first overtone bandhead of carbon
582 monoxide at high temperatures and high pressures, *Journal of Quanti-*
583 *tative Spectroscopy and Radiative Transfer* 239 (2019) 106636.
- 584 [29] J. P. Looney, G. J. Rosasco, Semiclassical calculation of self-broadening
585 in O₂, N₂, and CO Raman spectra, *J. Chem. Phys.* 95 (1991) 2379–2390.

Author Statement

Denís Paredes-Roibás: Writing, SRS Experiment.

Raúl Z. Martínez: Writing, SRS Experiment.

Franck Thibault: Writing, Calculations.

Journal Pre-proof

Declaration of interests

The authors declare that they have no known competing financial interests or personal relationships that could have appeared to influence the work reported in this paper.

The authors declare the following financial interests/personal relationships which may be considered as potential competing interests:

Journal Pre-proof